JOURNAL OF MATERIALS SCIENCE **34** (1999) 2331–2334

A new evaluation method of modal fracture energy of fiber-reinforced ceramic matrix composites

K. YASUDA, S. TANAKA*, Y. MATSUO
Department of Inorganic Materials, Faculty of Engineering, Tokyo Institute of Technology, 2-12-1 Ookayama, Meguro, Tokyo 152-8552, Japan
E-mail: tsatoshi@o.cc.titech.ac.jp

An evaluation method of modal fracture energy was newly proposed for fiber-reinforced ceramic matrix composites which essentially showed multi-modal fracture behavior. The total work done during fracture was separated into the tensile fracture work and the shear fracture work in consideration of the tensile fracture surface area and the shear fracture surface area. This modal separation resulted in the tensile fracture energy and the shear fracture energy per unit crack extension. Modal fracture energies of carbon fiber-reinforced pitch-derived carbon composites heat-treated at 1000 °C and 1200 °C were evaluated by this method. The tensile fracture energies of the composites heat-treated at 1000 °C and 1200 °C were 0.92 kJ/m^2 and 1.4 kJ/m^2, the shear fracture energies of the composites heat-treated at 1000 °C and 1200 °C were 0.020 kJ/m^2 and 0.030 kJ/m^2, respectively. The experimental result successfully demonstrated the adequate modal fracture energies of the composites.

1. Introduction

Fiber-reinforced ceramic matrix composites have been investigated to develop toughened ceramics for high temperature structural applications [1–9]. In the previous studies [3, 10], fracture behavior of the composites was characterized by the work of fracture. Since a projection area of a notch-ligament of a specimen was assumed to be a nominal fracture surface area, the work of fracture is valid if tensile fracture only takes place. However, the composites usually shows multi-modal fracture behavior (e.g., tensile fracture, shear fracture, compressive fracture) [11, 12], so that the work of fracture has less physical meaning. Therefore, it is necessary to evaluate each modal fracture energy separately.

The aim of the present study is to newly develop a method for evaluating modal fracture energy of fiber-reinforced ceramic matrix composites. At first, the fundamental concept of modal separation of fracture energy was proposed. Next, the single edge-notched beam tests were conducted on two types of carbon fiber-reinforced pitch-derived carbon composites (hereafter, C/C composites) heat-treated at 1000 °C and 1200 °C. Finally, the effectiveness of the new method was discussed with the experimental data.

2. Modal separation of fracture energy

Assume that a single edge-notched beam test was conducted on a rectangular cross-sectioned specimen as shown in Fig. 1. For simplicity, the specimen is assumed to be a unidirectional fiber-reinforced composite of which reinforcement aligned along the longitudinal direction of the specimen. During the test, it is supposed that tensile mode fracture and shear mode fracture simultaneously take place. Firstly, dissipated energies per unit crack extension during tensile fracture and shear fracture are defined as the tensile fracture energy γ_{tensile} and the shear fracture energy γ_{shear}. And the total fracture surface area S_{total} is defined as a sum of the tensile fracture surface area S_{tensile} and the shear fracture surface area S_{shear} as follows,

$$S_{\text{total}} = S_{\text{tensile}} + S_{\text{shear}} \tag{1}$$

The total work done during fracture, U_{WOF}, can be separated into the tensile fracture work $2\gamma_{\text{tensile}} S_{\text{tensile}}$, the shear fracture work $2\gamma_{\text{shear}} S_{\text{shear}}$ and the interaction energy $U_{\text{interaction}}$ as follows,

$$U_{\text{WOF}} = 2\gamma_{\text{tensile}} S_{\text{tensile}} + 2\gamma_{\text{shear}} S_{\text{shear}} + U_{\text{interaction}}(S_{\text{tensile}}, S_{\text{shear}}) \tag{2}$$

Dividing Equation 2 by $2S_{\text{total}}$ leads the following fundamental equation,

$$\frac{U_{\text{WOF}}}{2S_{\text{total}}} = \gamma_{\text{tensile}} \frac{S_{\text{tensile}}}{S_{\text{total}}} + \gamma_{\text{shear}} \frac{S_{\text{shear}}}{S_{\text{total}}} + \frac{U_{\text{interaction}}(S_{\text{tensile}}, S_{\text{shear}})}{2S_{\text{total}}}$$

* Author to whom all correspondence should be addressed.

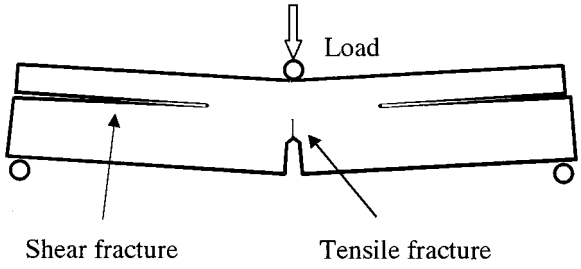

Figure 1 Multi-modal fracture behavior of fiber-reinforced ceramic matrix composite during a single edge-notched beam test.

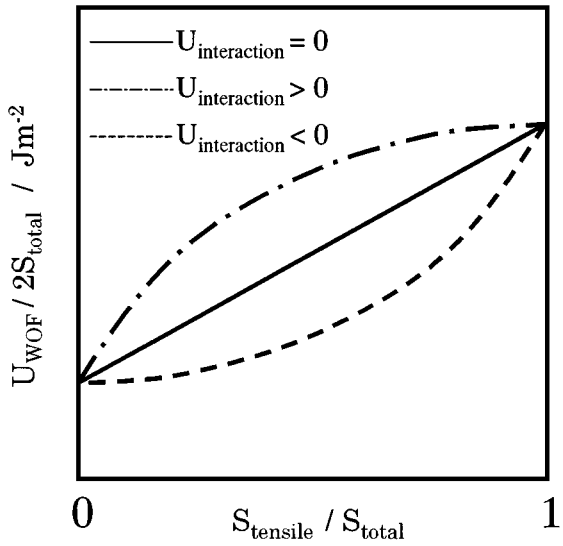

Figure 2 The relationship between $U_{WOF}/2S_{total}$ and $S_{tensile}/S_{total}$.

$$= (\gamma_{tensile} - \gamma_{shear})\frac{S_{tensile}}{S_{total}} + \gamma_{shear} + \frac{U_{interaction}(S_{tensile}, S_{shear})}{2S_{total}} \quad (3)$$

By plotting the experimental data on $U_{WOF}/2S_{total}$ versus $S_{tensile}/S_{total}$ diagram, we may obtain one of the curves as shown in Fig. 2. If there is no interaction between two fracture modes, the relation between $U_{WOF}/2S_{total}$ and $S_{tensile}/S_{total}$ should be a straight line with a slope of $(\gamma_{tensile} - \gamma_{shear})$ and y-intercept of γ_{shear}. If there is an interaction between two fracture modes, the line should be changed into convex or concave one. The tensile fracture energy $\gamma_{tensile}$ can be estimated from the value of $U_{WOF}/2S_{total}$ at $S_{tensile}/S_{total}$ being equal to 1. Similarly, the shear fracture energy γ_{shear} can be estimated from the value of $U_{WOF}/2S_{total}$ at $S_{tensile}/S_{total}$ being equal to 0. Needless to say, the number of fracture modes is not limited within two. This evaluation method can easily be expanded for multiple modes of fracture more than two.

3. Experimental

Uni-directional reinforced C/C composites heat-treated at 1000 °C and 1200 °C were used as the specimens, which were made by filament winding technique. PAN-based carbon fiber (TRAYCA T-300) and coal tar pitch (melting point: 85 °C, fixed carbon: 54%) were used as a reinforcement and a matrix precursor, respectively. Volume fraction of fiber in these composites were about 60%. Hereafter, the composites heat-treated at 1000 °C and 1200 °C are called HT10 and HT12, respectively.

TABLE I Characteristics of the used C/C composites

Specimen	Density (gcm^{-3})	Bulk density (gcm^{-3})	Apparent density (gcm^{-3})	Young's modulus (GPa)	Flexural strength (MPa)
HT10	1.79	1.38	1.59	100	180
HT12	1.81	1.41	1.59	120	190

Table I shows characteristics of the C/C composites. The bulk densities of the HT10 and the HT12 were 1.38 g/cm^3 and 1.41 g/cm^3, respectively. The apparent densities of the both composites were 1.59 g/cm^3. The densities of them were 1.79 g/cm^3 and 1.81 g/cm^3, respectively. Namely, the bulk density, the apparent density and the density were almost the same between two composites. The Young's modulus of the HT10 and the HT12 were 100 GPa and 120 GPa, respectively. The flexural strength of them were 180 MPa and 190 MPa, respectively. Namely, the Young's modulus and the flexural strength slightly increased with an increase in the heat-treatment temperature. It is considered that growth of graphite layers of matrix carbon resulted in the increase in the Young's modulus of the composites. We [13] have already reported the same tendency for the Young's modulus and the flexural strength of pitch-derived C/C composites. Therefore, the C/C composites prepared in this study have typical mechanical properties, and may be suitable samples for the research on modal separation of fracture energy.

As shown in Fig. 3, three types of specimens (type A:4 × 3 × 40 mm, type B:4 × 3 × 70 mm, type C:4 × 6 × 40 mm) were used for the single edge-notched beam tests to change contribution of fracture modes. A straight through notch was introduced into each specimen. The tip of a notch was finished with diamond slurry and a sharp blade to obtain a notch radius less than 20 μm. The relative notch length (hereafter a/W, where, a is the length of notch, W is the width of the specimen) was also changed from 1/4, 2/4 to 3/4 for all types of specimens. The single edge-notched beam tests were carried out with a Shimazu Autograph DCS-R-10TS under the cross-head speed of 0.5 mm/min until a specimen fractured completely. The span lengths were selected 30 mm for type A and type C, and 60 mm for type B.

4. Results and discussion

4.1. Fracture behavior of the C/C composites

Fig. 4 shows the typical load/displacement curves of the HT10 and the HT12 specimens in case of type A with an a/W of 2/4. Both curves depart from linearity before the load reaches to the maximum. After reaching the maximum, the load decreases gradually. Namely, both curves of the HT10 and the HT12 specimens exhibit the pseudo-ductile fracture behavior. The

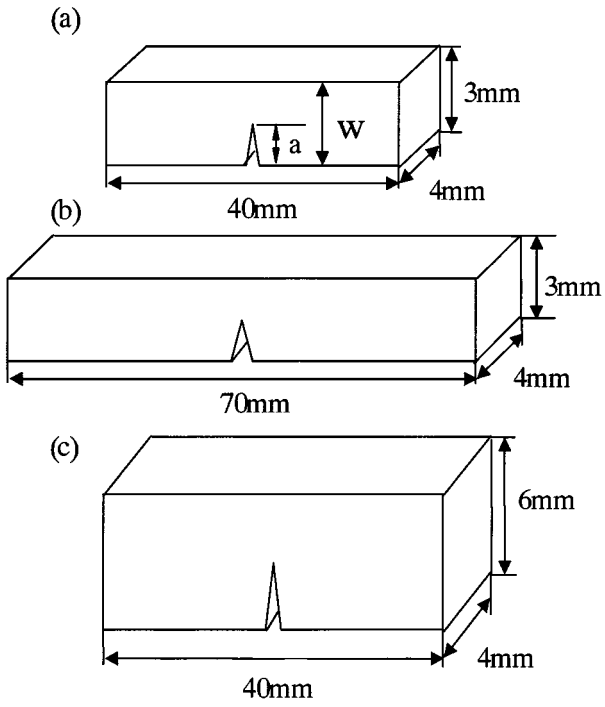

Figure 3 Dimensions of specimens for modal fracture energy measurement: (a) type A; (b) type B, and (c) type C.

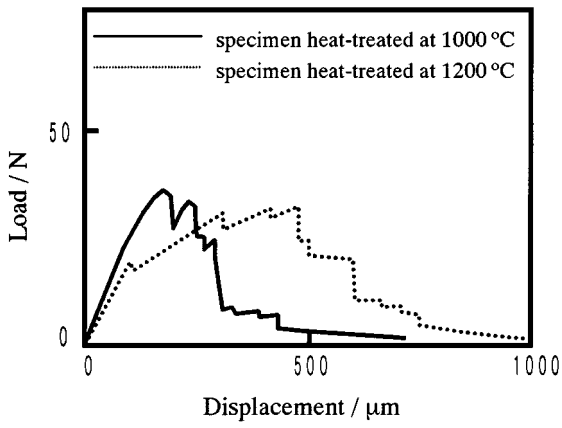

Figure 4 The load/displacement curves of type A with an a/W of 2/4.

typical appearances of both fractured specimens are shown in Fig. 5. Fracture behavior of the HT10 specimen is mostly tensile fracture, whereas that of the HT12 specimen is mixed with tensile fracture and shear fracture.

4.2. Evaluation of modal fracture energy for the C/C composites

The work done during fracture, U_{WOF}, is calculated from an area under the load/displacement curve. The tensile fracture surface area $S_{tensile}$ is given by multiplying the nominal ligament length $(W-a)$ and the breadth of the specimen. The shear fracture surface area S_{shear} is given by multiplying the observed length of shear cracks and the breadth of the specimen.

Fig. 6 shows the plots of $U_{WOF}/2S_{total}$ against $S_{tensile}/S_{total}$ for the HT10 and the HT12 specimens. Fig. 7 is an expanded view of Fig. 6 ranging from 0.0 to 0.2 of $S_{tensile}/S_{total}$. Although the type of the specimen

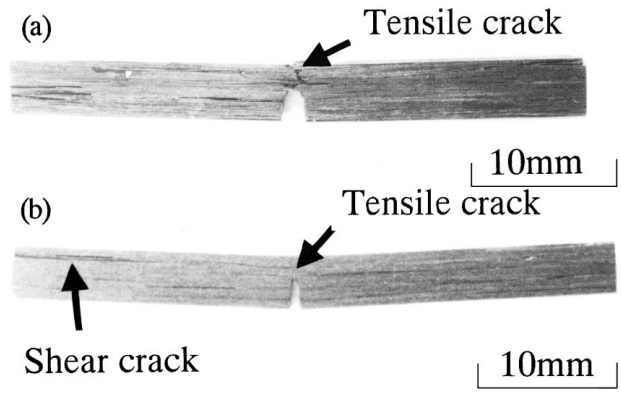

Figure 5 The appearance of type A after single edge-notched beam test: (a) specimen heat-treated at 1000 °C, (b) specimen heat-treated at 1200 °C.

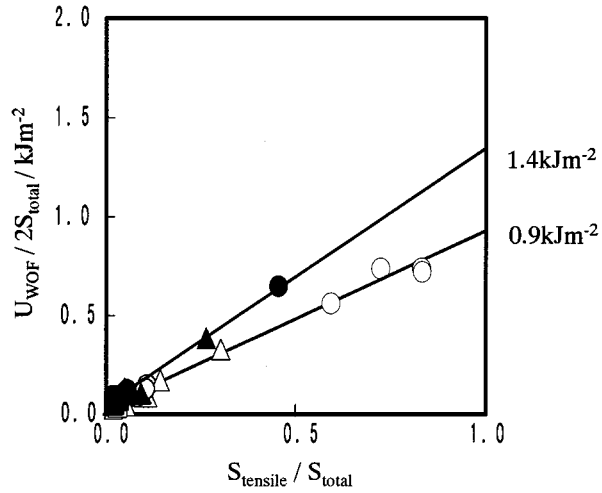

Figure 6 The relationship between $U_{WOF}/2S_{total}$ and $S_{tensile}/S_{total}$: ○: HT10 type A; △: HT10 type B; □: HT10 type C; ●: HT12 type A; ▲: HT12 type B; ■: HT12 type C.

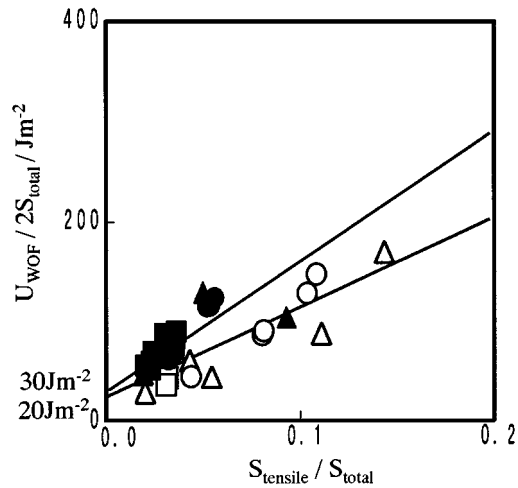

Figure 7 The expanded view of Fig. 6: ○: HT10 type A; △: HT10 type B; □: HT10 type C; ●: HT12 type A; ▲: HT12 type B; ■: HT12 type C.

and notch length are different, the relation between $U_{WOF}/2S_{total}$ and $S_{tensile}/S_{total}$ is almost on a linear line for each HT10 and HT12 specimen. Therefore, we conclude that modal separation of fracture energy is successfully demonstrated by the experimental result and there is no interaction between tensile fracture and shear

fracture for each the HT10 and the HT12 specimen. The regression lines for the HT10 and the HT12 specimens are also given in Fig. 6, respectively. The tensile fracture energy $\gamma_{tensile}$ and the shear fracture energy γ_{shear} are estimated from the extrapolative value of $U_{WOF}/2S_{total}$ at $S_{tensile}/S_{total}$ being equal to 1 and the extrapolative value of $U_{WOF}/2S_{total}$ at $S_{tensile}/S_{total}$ being equal to 0 in Fig. 6. Consequently, the tensile fracture energies $\gamma_{tensile}$ of the HT10 and the HT12 specimens are obtained to be 0.92 kJ/m^2 and 1.4 kJ/m^2, respectively, and the tensile fracture energy $\gamma_{tensile}$ of the HT12 specimens is larger than that of the HT10 specimens. Since the work of fracture of C/C composites were around several kJ/m^2 when the tensile fracture mainly occurred, it is considered that the tensile fracture energy $\gamma_{tensile}$ obtained in this study coincided well with the previous data [14]. The increase in tensile fracture energy $\gamma_{tensile}$ with heat-treatment temperature also corresponds to the same tendency of fracture toughness reported for polycrystalline graphite [15, 16]. On the other hand, the shear fracture energies γ_{shear} of the HT10 and the HT12 specimens are obtained to be 0.020 kJ/m^2 and 0.030 kJ/m^2, respectively, and the shear fracture energy γ_{shear} does not almost depend on the heat-treatment temperature. It can be explained by the weak Van der Waals force between the graphite layers in the pitch-derived C/C composites even if the heat-treatment temperature is as low as around 1000 °C. The above experimental data coincided with the tendencies in the previous studies. Thus, the experimental result shows the effectiveness for the evaluation method of modal fracture energy newly proposed here.

5. Conclusions

The following conclusions can be obtained in this study.

(1) An evaluation method of modal fracture energy was newly proposed for fiber-reinforced ceramic matrix composites which usually showed multi-modal fracture behavior. The total work done during fracture was separated into the tensile fracture work and the shear fracture work in consideration of the tensile fracture surface area and the shear fracture surface area. This modal separation resulted in the tensile fracture energy and the shear fracture energy per unit crack extension.

(2) Both modal fracture energies of C/C composites were evaluated by the new method. The tensile fracture energies of the composites heat-treated at 1000 °C and 1200 °C were 0.92 kJ/m^2 and 1.4 kJ/m^2, the shear fracture energies of the composites heat-treated at 1000 °C and 1200 °C were 0.020 kJ/m^2 and 0.030 kJ/m^2, respectively. The experimental result successfully demonstrated the effectiveness of the new evaluation method of modal fracture energy.

Acknowledgements

This research was partly supported by Grants from the Grant-in-Aid for Scientific Research (No.09750760) from the Japan Ministry of Education, Science and Culture, and the Grant-in-Aid for JSPS Fellows (No.4458), and Ishikawa Foundation for Carbon, Science and Technology.

References

1. R. A. SAMBELL, D. H. BROWEN and D. C. PHILLIPS, *J. Mater. Sci.* **7** (1972) 663–675.
2. R. A. SAMBELL, A. BRIGGS, D. C. PHILLIPS and D. H. BOWEN, *ibid.* **7** (1972) 676–681.
3. D. C. PHILLIPS, *ibid.* **7** (1972) 1175–1191.
4. J. K. DUO, Z. Q. MAO, C. D. BAO, R. H. WANG and D. S. YAN, *ibid.* **17** (1982) 3611–3636.
5. K. M. PREWO and J. J. BRENNAN, *ibid.* **15** (1980) 463–468.
6. J. J. BRENNAN and K. M. PREWO, *ibid.* **17** (1982) 2371–2383.
7. T. YAMAMURA, T. ISHIKAWA, M. SHIBUYA, M. TAMURA, H. OHTSUBO, T. NAKAZAWA and K. OKAMURA, in Proc. 1st Japan Int. SAMPE Symposium, 1989, pp. 1084–1089.
8. K. NAKANO, A. KAMIYA, M. IWATA and K. OSHIMA, *ibid.*, 1989, pp. 1090–1095.
9. M. IWATA, *J. Jpn. Soc. Powder Powder Metallur.* **37** (1990) 1108–1112.
10. M. JEKINS, J. MIKAMI, T. CHANG and A. OKURA, *Trans. Jpn. Ins. Metal* **29**(7) (1988) 573–579.
11. S. KIMURA, K. YASUDA, E. YASUDA and Y. TANABE, *Tanso* (1987) 30–37.
12. S. KIMURA, A. HOTTA, S. OSAWA, K. YASUDA and Y. MATSUO, *ibid.* (1992) 288–294.
13. S. KIMURA, E. YASUDA, K. YASUDA, Y. TANABE, K. KAWAMURA and M. INAGAKI, *ibid.* (1988) 62–68.
14. M. SAKAI, T. MIYAJIMA and M. INAGAKI, *Compo. Sci. Technol.* **40** (1991) 231–250.
15. M. KANO, Y. MATSUO and K. YASUDA, Ext. Abst. of the Annual Meeting of Carbon Society of Japan, Tokyo, 1994, pp. 252–253.
16. K. AHLBORN, T. CHOU, Y. KAGAWA and A. OKURA, *Carbon* **32**(1) (1993) 205–212.

Received 21 October
and accepted 16 November 1998